J Ind Microbiol Biotechnol (2013) 40:235–244
DOI 10.1007/s10295-012-1215-9

Distribution of live and dead cells in pellets of an actinomycete *Amycolatopsis balhimycina* and its correlation with balhimycin productivity

Kamaleshwar P. Singh · Amit L. Mahendra · Vibha Jayaraj · Pramod P. Wangikar · Sameer Jadhav

Received: 28 August 2012 / Accepted: 2 November 2012 / Published online: 27 November 2012

Abstract Secondary metabolites such as antibiotics are typically produced by actinomycetes as a response to growth limiting stress conditions. Several studies have shown that secondary metabolite production is correlated with changes observed in actinomycete pellet morphology. Therefore, we investigated the correlation between the production of balhimycin and the spatio-temporal distribution of live and dead cells in pellets of *Amycolatopsis balhimycina* in submerged cultures. To this end, we used laser scanning confocal microscopy to analyze pellets from balhimycin producing and nonproducing media containing 0.2 and 1.0 g l^{-1} of potassium di-hydrogen phosphate, respectively. We observed a substantially higher fraction of live cells in pellets from cultures yielding larger amounts of balhimycin. Moreover, in media that resulted in no balhimycin production, the pellets exhibit an initial death phase which commences from the centre of the pellet and extends in the radial direction. A second growth phase was observed in these pellets, where live mycelia are seen to appear in the dead core of the pellets. This secondary growth was absent in pellets from media producing higher amounts of balhimycin. These results suggest that distribution of live and dead cells and its correlation with antibiotic production in the non-sporulating *A. balhimycina* differs markedly than that observed in *Streptomycetes.*

Keywords Microbial fermentation · Confocal microscopy · Mycelial morphology · Antibiotic production

K. P. Singh
Department of Biosciences and Bioengineering, Indian Institute of Technology Bombay, Powai, Mumbai 400076, India

A. L. Mahendra · V. Jayaraj · P. P. Wangikar · S. Jadhav (✉)
Department of Chemical Engineering, Indian Institute of Technology Bombay, Powai, Mumbai 400076, India
e-mail: srjadhav@che.iitb.ac.in

Introduction

Commercial-scale production of secondary metabolites is usually carried out in submerged microbial cultures, operated in batch or fed-batch mode. Cost-effective production usually requires the product titer be maximized which may be attained by classical strain improvement procedures combined with process optimization strategies [3, 4, 38]. In order to ensure consistent end-of-batch productivity, the process parameters such as medium composition, temperature, pH and concentration of dissolved oxygen require close monitoring and tight control about their optimal values [16]. An early prediction of batch behaviour can help in some cases to take corrective steps, in a timely manner, towards rescuing a batch, or in others, to quickly terminate a potentially irredeemable batch thereby limiting the losses in raw material and utilities.

A significant fraction of commercially important secondary metabolites are produced by a group of gram-positive filamentous bacteria known as actinomycetes [5, 14, 35]. In addition, actinomycetes play an important role in carbon recycling in the natural habitat, since they are capable of degrading lignocellulose from dead plant material [29, 30]. Clinically important compounds such as antibiotics are typically produced by actinomycetes as a response to growth limiting stress conditions such as nutrient limitation and high cell densities [6, 9]. For instance, the repression of secondary metabolite production in actinomycetes by glucose and inorganic phosphate are well-known [9, 15, 28]. In fact, several studies with *Streptomycetes* have focused on delineating the relevant molecular mechanisms by which glucose or inorganic phosphate regulate secondary metabolism [6, 27, 42].

Submerged cultures of actinomycetes exhibit diverse morphological forms [17] that are modulated by

environmental factors within the fermentor including medium composition and fluid mechanical forces [7, 10, 33, 39]. Moreover, several works have reported that the morphological forms existing within a culture are correlated to the amount of antibiotic produced. For instance, morphology and avermenctin production by *Streptomyces averminitilis*, were shown to be influenced by factors such as the nitrogen source, dissolved oxygen level and inoculum volume [41]. It was reported that pellets of small size and high density promote avermenctin production. Similarly, nystatin production was correlated with smaller pellets of *Streptomyces noursei* NG7.19 [15]. Several works by Sanchez and coworkers have been directed towards studying the distribution of live and dead cells in pellets of *Streptomycetes* during the developmental cycle in solid (surface) and liquid (submerged) cultures [20–23, 25, 26]. They report that the production of antibiotics, undecylprodigiosin and actinorhodin, in submerged cultures of *Streptomyces coelicolor* A3(2) commences following a transient growth arrest, and antibiotic appearance correlates strongly with the development of a second, multinucleated, mycelium [20]. In fact, in diluted-inoculum cultures, antibiotic production was delayed until the second mycelium was formed.

In our previous work, we characterized the effect of varying concentrations of KH_2PO_4 and ammonium sulfate in defined media and in industrially relevant complex media on pellet morphology for the actinomycete *Amycolatopsis balhimycina* DSM 5908, which produces balhimycin, a glycopeptide antibiotic [36]. We reported that higher balhimycin productivity is correlated with higher pellet to dispersed mycelia ratio in the biomass, small elongated pellets as well as shorter filaments in peripheral hyphae of the pellets. In the present work, we investigated the correlation between the live and dead cell distribution in pellets of *A. balhimycina* in submerged cultures with the production of balhimycin. To this end, we used laser scanning confocal microscopy (LSCM) to analyze pellets from seed medium as well as balhimycin producing and non-producing defined media containing 0.2 and 1.0 g l^{-1} of KH_2PO_4, respectively. Our observations correlating antibiotic production to the temporal and spatial distribution of live and dead cells in pellets of *A. balhimycina* differ markedly from those reported in previous studies with *Streptomycetes*.

Materials and methods

Materials

Yeast extract (YE), meat extract, dextrose, peptone, agar powder, MES buffer, Bennet's agar and vitamins were purchased from Hi-Media laboratories (Mumbai, India) whereas glycerol, $(NH_4)_2SO_4$ (AMS), NaCl, $MgSO_4{\cdot}7H_2O$, $FeSO_4{\cdot}7H_2O$, $Na_3(C_6H_5O_7){\cdot}2H_2O$, $ZnSO_4{\cdot}7H_2O$, $MnSO_4{\cdot}H_2O$, $CaCl_2{\cdot}2H_2O$ were purchased from Merck (Mumbai, India). Soya peptone and $CaCO_3$ were purchased from Micro Master Laboratories Pvt. Ltd. (Thane, India) and S.D. Fine Chemicals (Mumbai, India) respectively. The KH_2PO_4 was purchased from Thomas Baker, Chemical Ltd. (Mumbai, India). Balhimycin standard was a kind gift from Prof. Anna Eliasson Lantz, Denmark's Technical University, Denmark.

Inoculum preparation and fermentation

Amycolatopsis balhimycina was a kind gift from Prof. Anna Eliasson Lantz, Denmark's Technical University, Denmark. The strain was cultivated and maintained as reported previously [18, 19]. The inoculum was prepared in 500 ml single baffled Erlenmeyer flasks containing 100 ml of seed medium. The seed medium contained 15.0 dextrose, 15.0 g l^{-1} glycerol, 5.0 g l^{-1} YE, 15.0 g l^{-1} soya peptone and 3.0 g l^{-1} sodium chloride.

The fermentations were carried out in shake flasks as well as in a bioreactor. Shake flask fermentations were performed in 500 ml single baffled Erlenmeyer flasks containing 100 ml of production medium whereas the bioreactor fermentations were carried out in a 2.0 l bioreactor containing 1.0 l of production medium. Shake flasks and the bioreactor were inoculated with 2.5 % (v/v) of seed culture having an optical density of $\sim$12.0 at 600 nm and the temperature was maintained at 30 °C. For shake flasks the speed of the shaker was kept at 150 rpm. Bioreactor pH was maintained at 7.0 by using 1.5 N NaOH and 1.5 N H_2SO_4 solutions. The bio-reactor was aerated at a flow rate of 1.0 vvm (volume of air per unit volume of medium per minute) using a mass flow controller. Dissolved oxygen (DO) concentration in the bio-reactor was maintained at 40 % of saturation value by regulating the stirrer speed with a PID controller. The lower and upper bounds of stirrer speed were fixed at 150 and 500 rpm, respectively.

In the present study, the production medium used in shake flasks as well as bioreactor was the same, comprising of either 0.2 or 1.0 g l^{-1} KH_2PO_4, 80.0 g dextrose, 6.6 g $(NH_4)_2SO_4$, 1.0 g NaCl, 1.5 g $MgSO_4{\cdot}7H_2O$, 0.02 g $FeSO_4{\cdot}7H_2O$, 0.025 g $Na_3(C_6H_5O_7){\cdot}2H_2O$, 0.02 g $ZnSO_4{\cdot}7H_2O$, 0.01 g $MnSO_4{\cdot}H_2O$, 0.01 g $CaCl_2{\cdot}2H_2O$, 9.762 g MES, 11.0 g $CaCO_3$ and 1 ml vitamin solution (1000X) per liter of distilled water. The 1000X vitamin stock solution contained, per 100 ml of distilled water: 0.005 g biotin, 0.1 g calcium-pantothenate, 0.1 g nicotinic acid, 2.5 g myo-inositol, 0.1 g thiamin HCl, 0.1 g pyridoxine HCl and 0.02 g para-amino benzoic acid. Samples were collected from the seed and production media at regular intervals for microscopic analysis as well as balhimycin, biomass, dextrose, glycerol and ammonium sulfate estimation. Data were represented as mean $\pm$ SEM obtained from three independent experiments.

Estimation of biomass, dextrose, glycerol and ammonium sulfate

Samples were taken from the fermentation medium from the shake flask and the bioreactor at regular intervals to analyse biomass, dextrose, glycerol and ammonium sulfate as described earlier [2, 19]. Dextrose and glycerol were estimated by using a HP-Aminex- 87-H column (Bio-Rad, Hercules, USA) where the mobile phase consisting of 5 mM sulfuric acid in water was perfused at 0.6 ml per minute. The temperature of the column was maintained at 65 °C. Separated components were detected by using a RI detector (L-7490, Merck HITACHI KGaA, Darmstadt, Germany). Ammonia was estimated using Nessler's reagent [31].

Estimation of balhimycin

Concentration of balhimycin in fermentation broth obtained from both the shake flask and the bioreactor was estimated using a bioassay and further confirmed via HPLC as previously described [1, 18, 19, 36]. In the bioassay, *Kocuria rhizophila* ATCC9341, old name *Micrococcus luteus* [37], was used as a test organism to measure antimicrobial activity of balhimycin. For this purpose, Petri plates were poured with agar containing the test organism. Ten mm diameter holes were punched in the agar and filled with 0.1 ml sample of the centrifuged fermentation broth. The plates were incubated at 30°C for two days and the diameter of zone of inhibition around the holes was measured. The balhimycin concentration was estimated using a standard calibration curve. Balhimycin concentration was confirmed for some time points by HPLC using a RP-C_{18} column (Merck KGaA Darmstadt, Germany) and a mobile phase (1 ml/min.) consisting of 18 % of acetonitrile and 0.1 % of TFA (Trifluoro acetic acid) in water. Separated components were detected at 220 nm wave length using L-7420 UV detector (Merck Hitachi KGaA, Darmstadt, Germany) [32]. Balhimycin concentration estimated by HPLC was not significantly different from the bioassay-based measurements (data not shown).

Estimation of dispersed and pellet form

The dispersed mycelia and pellets in the culture broth were estimated as detailed in an earlier study [36]. Briefly, samples taken from shake flask or bioreactor were observed using an inverted microscope (TE-2000, Nikon, Tokyo, Japan) and images were captured with a CCD camera (Retiga-2000R, QImaging, Surrey,Canada). The images were analyzed using the software ImageJ 1.40 g (http://rsb.info.nih.gov/ij/) [8]. Mycelial aggregates first enclosed into a best fit circle (or ellipse), and subsequently the radius of the circle (or major axis and minor axis of the ellipse) was measured. The dispersed mycelia or pellets were assumed to be spheres or prolate ellipsoids for volume estimation. When volume enclosed was less than 5×10^4 μm^3, these were assumed to be dispersed mycelia. Pellets were those with volume equal to or greater than 5×10^4 μm^3. Nearly 300 events were counted per time point per experiment with data represented as the mean ± SEM of three independent experiments.

Live/dead cell staining and confocal/epi-fluorescence microscopy

To examine the distribution of live and dead cells in *A. balhimycina* pellets, we used the *LIVE/DEAD Bac-Light* bacterial viability kit (L-13152, Invitrogen) containing two nucleic acid staining dyes, propidium iodide (PI) and SYTO 9 [11, 12, 22]. The SYTO 9 is a green fluorescent dye which enters live as well as dead cells. In contrast, PI penetrates only dead cells with damaged membranes. PI has a higher affinity for the nucleic acids and displaces SYTO 9 in dead cells. Therefore, in the presence of both stains, bacteria with intact cell membranes appear fluorescent green whereas bacteria with damaged membranes appear red.

Biomass samples drawn at different time points from the culture broth of bioreactor were centrifuged, washed twice and re-suspended in saline (0.9 % NaCl). The nucleic acid stains were prepared and mixed at concentrations recommended by the manufacturer. Next, equal volumes (20 µl) of stain mixture and sampled mycelia suspension were mixed on a clean slide [11]. A cover slip was placed over the sample and kept for 10 min in the dark prior to microscopic analysis. The samples, analyzed using a laser-scanning confocal/epi-fluorescence microscope (LSM510, Zeiss, Jena, Germany), were sequentially excited at wavelengths of 488 nm and 568 nm and observed at emission wavelengths of 530 nm (green) and 630 nm (red), respectively. The green and red fluorescence of the pellets was quantified using the software provided by the manufacturer (Zeiss, Jena, Germany). On an average the ratio of green to red fluorescence of 20 pellets was estimated for each time point and data was represented as the mean ± standard deviation. For each time point, more than 15 images were analyzed which were pooled from three independent experiments.

Results

A rigorous study on the correlation between pellet morphology of *A. balhimycina* and balhimycin production has been described previously [36]. In the current study, our objective was to study the fraction of live and dead cells in

mycelia that result in balhimycin production. To this end, we selected two defined media differing only in KH_2PO_4 concentrations: a high balhimycin producing medium containing 0.2 g l^{-1} of KH_2PO_4 and a nonproducing medium containing 1.0 g l^{-1} of KH_2PO_4 [18]. For the sake of completeness we also chose the seed media in this study. In the previous studies [36], balhimycin fermentation was carried out in shake flasks where calcium carbonate was used to prevent excursions of pH in the acidic range. During sample preparation for microscopy, 2 ml of 2 N hydrochloric acid was added to 5 ml culture broth to dissolve the solid particles of calcium carbonate. While this did not affect image analysis for phase contrast microscopy, severe artifacts were observed for imaging with confocal laser scanning microscopy (CLSM). Specifically, when the samples were stained for live/dead cell analysis with the fluorophores SYTO 9 and PI, red fluorescence representing dead mycelium was observed over the entire pellet. We ascribed this artifact to the possible degradation of live cell plasma membrane by hydrochloric acid. Therefore, to avoid the use of calcium carbonate during fermentation and in turn hydrochloric acid during sample preparation, balhimycin fermentation was carried out in a bioreactor where pH was controlled with a PID controller using sodium hydroxide (1.5 N) and sulfuric acid (1.5 N). Stirrer speed was controlled to maintain the dissolved oxygen (DO) level at 40 %. Samples taken at different time points were stained with SYTO 9 and PI, and subsequently imaged using confocal microscopy (for details see the "Materials and methods" section).

Biomass and product formation, substrate uptake and mycelial morphology in bioreactor and shake flask

As a first step, we confirmed that biomass formation in the bioreactor was similar to that observed in the shake flask experiments in seed medium as well as in production media containing 0.2 and 1 g l^{-1} of KH_2PO_4. In the case of seed medium as well as production medium containing 0.2 g l^{-1} of KH_2PO_4, the rate of biomass formation was marginally higher in the bioreactor when compared to that in shake flask experiments (Fig. 1a, b). For production medium containing 1.0 g l^{-1} of KH_2PO_4, the rate of biomass production was similar in the bioreactor and shake flask (Fig. 1c). The rate of dextrose uptake in seed medium was similar in the bioreactor and the shake flasks (Fig. 1a), while in the case of production media, the same was observed to be slightly faster in the bioreactor compared to the shake flasks (Fig. 1b, c). Glycerol consumption rate in seed medium (Fig. 1a) as well as ammonium sulfate uptake rate in production media was also found to be marginally higher in the bioreactor compared to that in the shake flask experiments (Fig. 1b, c). As observed in the shake flask experiments, balhimycin production was

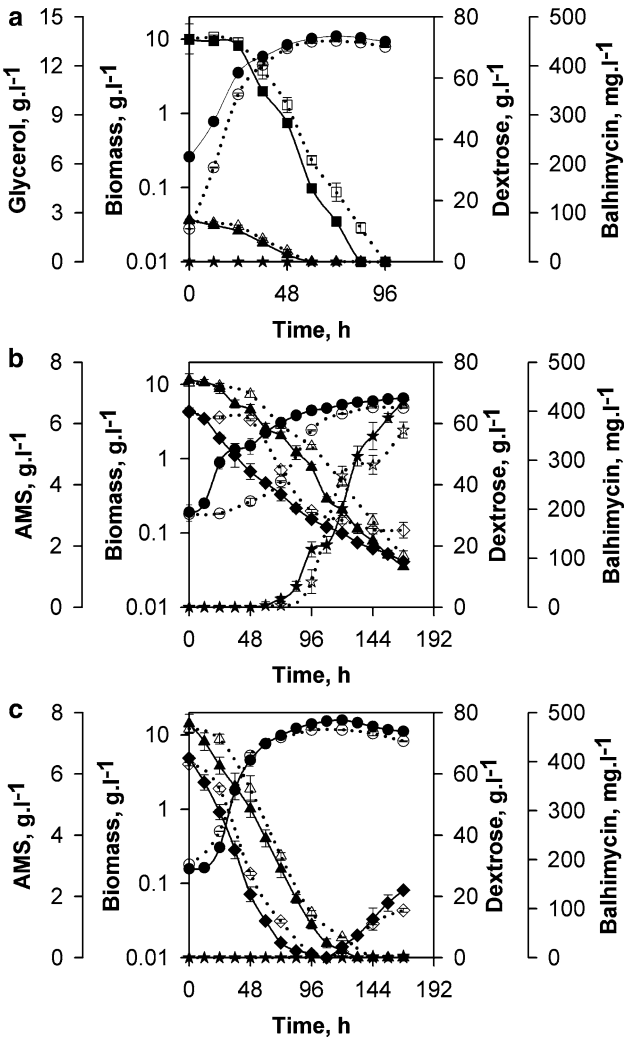

Fig. 1 Biomass growth, substrate uptake and balhimycin production in shake flask and bioreactor. Rates of biomass growth (*circle*), balhimycin production (*star*), and uptake rates of glycerol (*square*), dextrose (*triangle*) and ammonium sulfate (AMS, *diamond*) were estimated in a shake flask (*dotted lines* with *open symbols*) and a bioreactor (*solid lines* with *solid symbols*) for seed medium (**a**) as well as defined medium containing 0.2 g.l^{-1} of KH_2PO_4 (**b**) and 1.0 g.l^{-1} of KH_2PO_4 (**c**). Data represented as mean ± SEM obtained from three independent experiments

not detected in seed medium as well as in production medium containing 1.0 g l^{-1} of KH_2PO_4 when the bioreactor was used (Fig. 1a, c). In the case of production medium containing 0.2 g l^{-1} of KH_2PO_4, balhimycin production commenced slightly earlier in the case of the bioreactor compared to the shake flasks (Fig. 1c). Taken together, depending on medium composition, rates of biomass formation, substrate uptake and commencement of product formation in the bioreactor were similar or only slightly faster than those observed in shake flasks which may be attributed to more efficient mass transfer in the bioreactor.

Our previous shake flask experiments showed that in contrast to seed medium as well as nonproducing medium

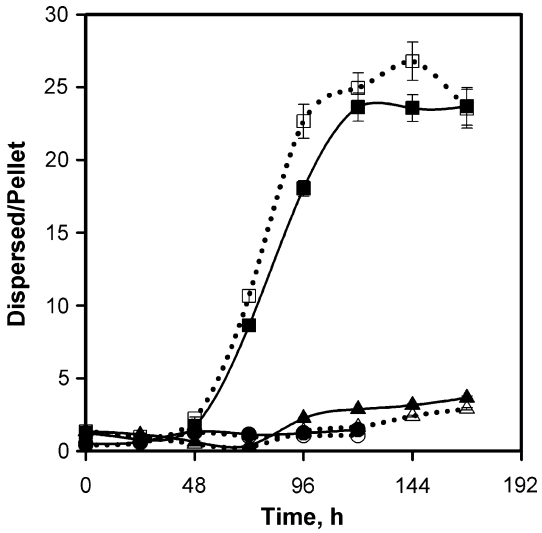

Fig. 2 Ratio of dispersed mycelia to pellets for *A. balhimycina* cultured in shake flask and bioreactor. Relative fractions of dispersed mycelia to pelleted were estimated in samples taken from shake flask (*dotted line* with *open symbol*) and bioreactor (*solid line* with *solid symbol*). Experiments were carried out in seed medium (*circle*) as well as defined medium containing 0.2 g.l^{-1}(*triangle*) and 1.0 g.l^{-1} (*square*) KH_2PO_4. Data represented as the mean ± SEM obtained from three independent experiments with a population size of ~300 events per time point per experiment

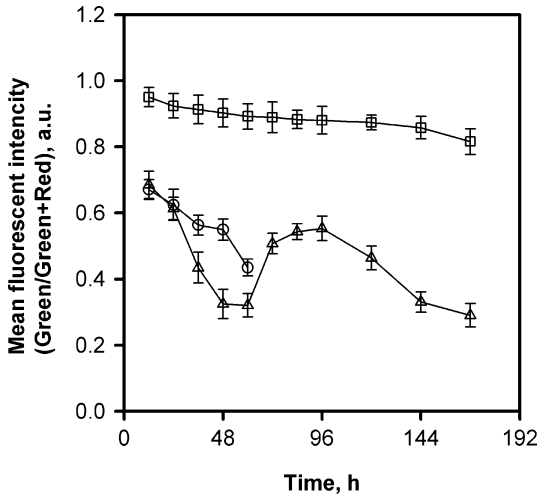

Fig. 3 Fraction of live mycelia in pellets of *A. balhimycina.* The fraction of live mycelia in pellets of *A. balhimycina* cultured in seed medium (*circle*) as well as defined media containing 0.2 (*square*) and 1.0 g.l^{-1} (*triangle up*) KH_2PO_4 in bioreactor were estimated from the ratio of *green* to total (*green* + *red*) fluorescence intensity of a single pellet. On an average the data obtained from 20 pellets were represented as mean ± SD

containing 1.0 g l^{-1} of KH_2PO_4, where pellets of *A. balhimycina* were large and spherical, those observed in high balhimycin producing medium containing 0.2 g l^{-1} of KH_2PO_4 were relatively small and elongated [36]. In seed as well as in production media, pellet morphologies observed in bioreactor experiments were similar to those in shake flasks (data not shown). We also compared the ratio of dispersed mycelia to pellets in biomass during bioreactor and shake flask fermentation. For the 72 h time point and later, the ratio of dispersed mycelia to pellets was substantially larger in production media containing 1.0 g l^{-1} of KH_2PO_4 compared to seed and producing medium containing 0.2 g l^{-1} of KH_2PO_4 in the shake flasks as well as the bioreactor (Fig. 2). Altogether, we conclude that the morphological differences in *A. balhimycina* due to different media conditions in the bioreactor closely resembled those captured in the shake flask experiments.

Effect of medium composition on fraction of live and dead cells in pellets

As an estimate of the fraction of live cells in pellets observed in seed as well as defined medium containing 0.2 and 1.0 g l^{-1} of KH_2PO_4, the total green fluorescence was normalized with the sum of green and red fluorescence intensity for each pellet. In the case of seed medium, the fraction of green fluorescence to total fluorescence decreased rapidly and steadily from 0.68 at 12 h to 0.43 at 60 h (Fig. 3). Taken together with the observation that biomass continued to increase till 60 h of seed culture (Fig. 1a), cell growth and death seem to be occurring simultaneously at an appreciable rate. In case of medium containing 1.0 g l^{-1} of KH_2PO_4 which did not produce balhimycin, the fraction of live cells decreased much more rapidly from 0.68 at 12 h to 0.32 at 48 h (Fig. 3), while total biomass continued to increase in this time interval (Fig. 1b). This indicated the simultaneous increase in the number of live and dead cells in pellets of *A. balhimycina*. Interestingly, after 60 h, the fraction of live cells started to increase till 96 h to a value of 0.57, indicating a second growth phase, distinct from the first (Fig. 3). After the 96 h time point the fraction of live cells again decreased till the end of the batch at 168 h to a final value of 0.3 (Fig. 3). In contrast to seed culture and media that did not produce balhimycin, the fraction of live cells in the high balhimycin producing medium containing 0.2 g l^{-1} of KH_2PO_4 was at a significantly higher value of 0.9 at 12 h and decreased at a very slow rate to 0.82 at 168 h (Fig. 3).

Spatio-temporal distribution of live and dead cells in the pellets of seed medium

Since the inoculum was cultured in seed medium for 48 h prior to transferring into defined media, we first examined the spatial distribution of live and dead cells in pellets from the seed medium up to 60 h. At the 12 h time point, pellets of *A. balhimycina* were observed to be spherical with a small inner core of dead mycelia surrounded by predominantly live mycelia at the periphery (Fig. 4a). As the size of

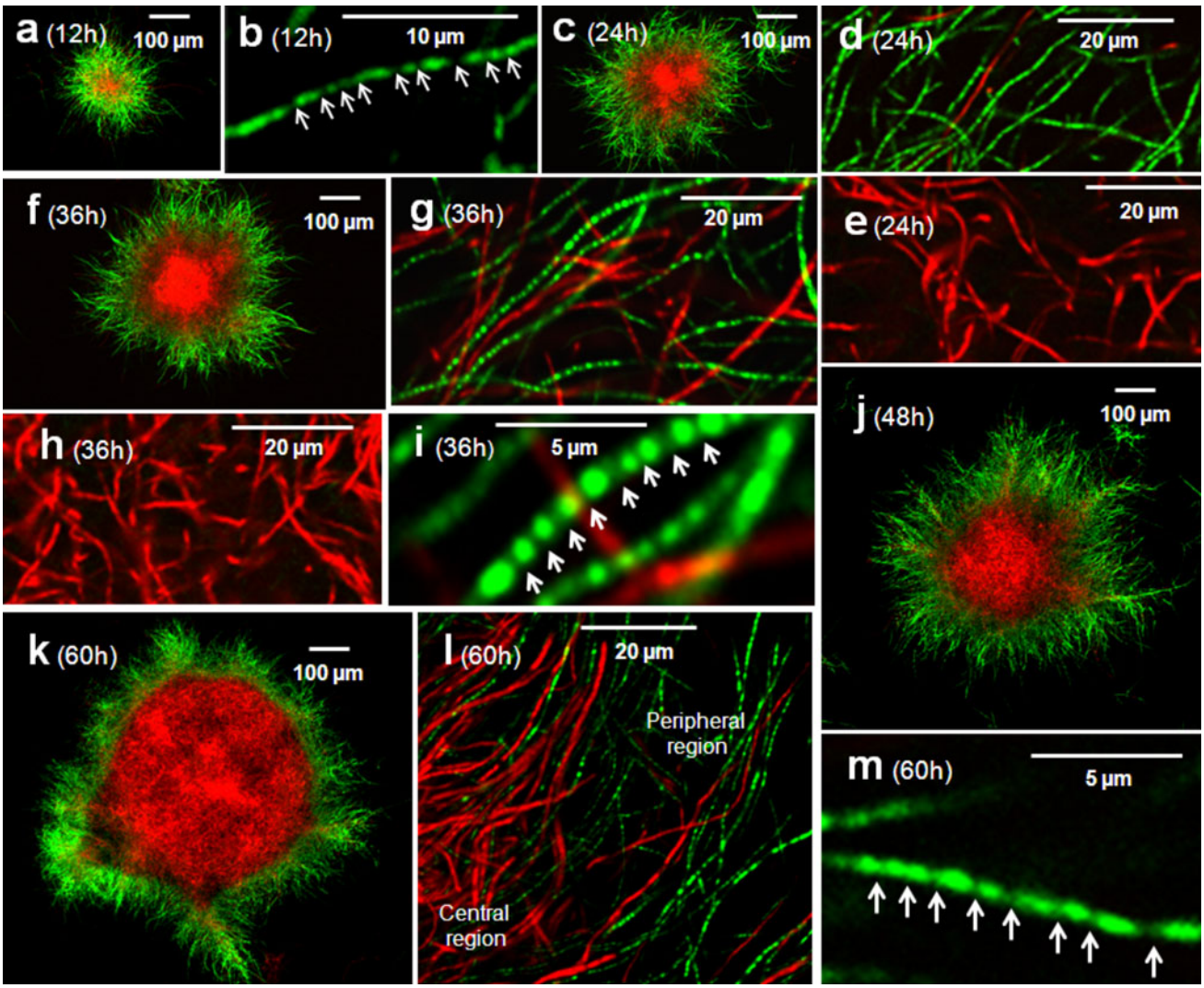

Fig. 4 Confocal laser scanning microscopy (CLSM) of live and dead cells in pellets of *A. balhimycina* grown in seed medium. Samples were collected at 12 h intervals from the bioreactor and stained with SYTO 9 and PI to identify live and dead cell, respectively (details in "Materials and methods" section). *Sample time point* (hours) and *scale bar* (micrometers) are indicated in each figure (**a**–**m**). **d** and **g** represent peripheral mycelial structure of the pellet at 24 h (**c**) and 36 h (**f**), respectively, whereas **e** and **h** are the central mycelial core of the pellet at 24 h (**c**) and 36 h (**f**), respectively. **l** represents central and peripheral mycelial structure of pellet at 60 h (**k**). *Arrows* in **b**, **i** and **m** show position of septa inside the live mycelia

the pellets increased with time (Fig. 4a, c, f, j, k), the central core of dead cells was found to grow at a relatively faster rate and a major fraction of the pellet consisted of dead cell mass by the 60 h time point (Fig. 4k). Moreover, observations at higher magnification revealed that the central core consisted of only dead cell mass (Fig. 4e, h, l) whereas peripheral region contained both live and dead hyphae (Fig. 4d, g, l). High magnification micrographs of the live hyphae at 12, 36 and 60 h time points (Fig. 4b, i, m), revealed separation of nucleoids and showed that the septation pattern of hyphae did not change over the entire duration of seed culture. Taken together, as the pellets in the seed medium grew in size, cell death was initiated from the center of the pellet and appeared to overtake the rate of pellet growth.

Distribution of live and dead cells in pellets of medium containing 0.2 g l^{-1} KH_2PO_4

In contrast to pellets observed in seed medium (Fig. 4), relatively small and elongated pellets were observed in the high balhimycin producing medium containing 0.2 g l^{-1} of KH_2PO_4, with a modest to moderate increase in pellet size over time (Fig. 5a, b, d, e, g, h, k–o). The Live/dead cell assay showed that almost all the cells in the pellets are alive and a very small fraction of dead cells are observed

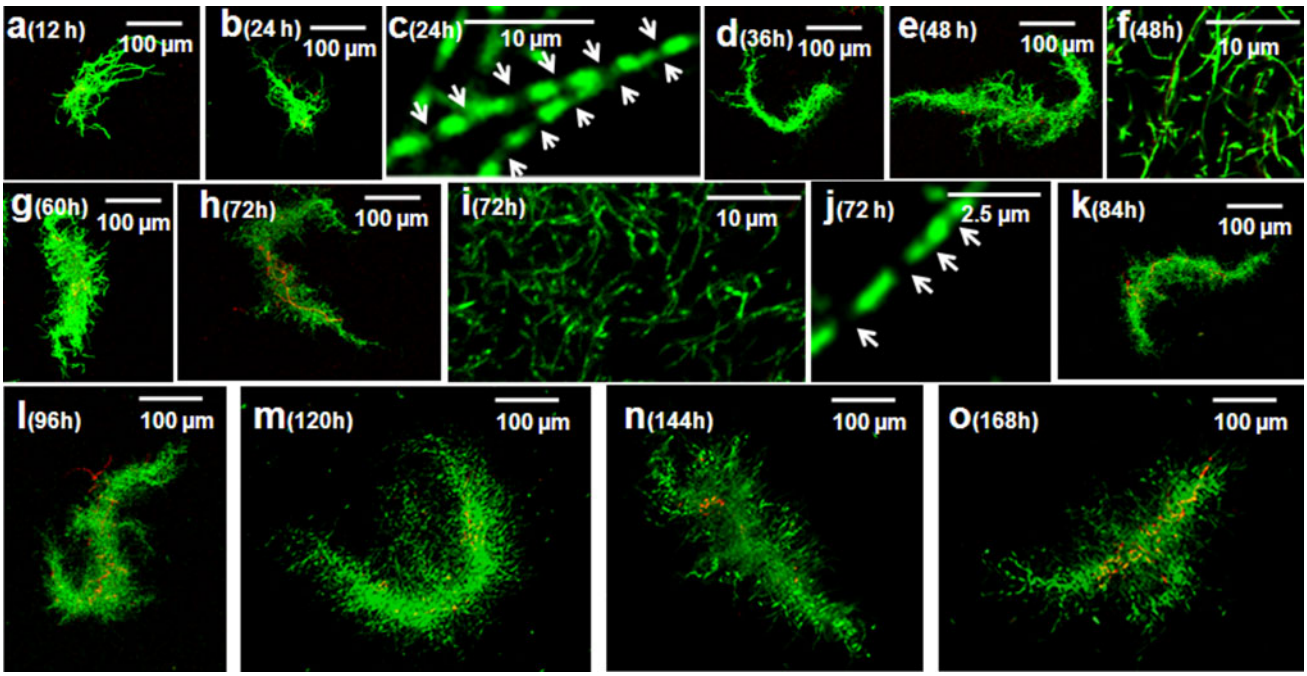

Fig. 5 Confocal and epi-fluorescence micrographs of live and dead cells in pellets of *A. balhimycina* cultured in medium containing 0.2 g l^{-1} of KH_2PO_4. Samples were collected at 12 h intervals from the bioreactor and stained with SYTO 9 and PI to identify live and dead cells, respectively (details in "Materials and methods" section). *Sample time point* (hours) and *scale bar* (micrometers) are indicated in each figure (**a**–**o**). **f** and **i** represent mycelial structure in pellets at 48 h (**f**) and 72 h (**j**), respectively. *Arrows* in (**c**) and (**j**) indicate position of septa inside the live mycelia

over the time course of the culture (Fig. 5). Imaging at higher magnification confirmed that the hyphae consisted almost entirely of live cells (Fig. 5f, i). A marginal increase in the fraction of dead cells was observed only toward the end of the batch at 168 h (Fig. 5o). High magnification micrographs showed separated nucleoids in the hyphae at 24 h, (Fig. 5c) and the septation pattern did not change with time as observed from images taken at the 72 h time point (Fig. 5j). Overall, our observations suggest that the pellets in high balhimycin producing medium grow slowly with an inappreciable rate of cell death.

Distribution of live and dead cells in pellets of medium containing 1.0 g l^{-1} KH_2PO_4

As was previously observed in shake flask experiments [36], with medium containing 1.0 g l^{-1} of KH_2PO_4, which did not yield balhimycin, large and spherical pellets were the dominant population in the bioreactor as well (Fig. 6). Similar to pellets of seed medium, cellular death started before 12 h at the center of the pellets from the nonproducing medium and the core of dead mycelia grew till it reached the peripheral boundary of pellets till the 60 h time point (Fig. 6a, b, f, g, h). At the 24 h time point, the central core of the pellet contained only dead cell mass (Fig. 6c) while the peripheral region was comprised of only live mycelia (Fig. 6d). Moreover, similar to observations in the seed medium (Fig. 4), as the pellets from the nonproducing medium grew, an inner core of dead cells grew at a relatively faster rate till 60 h where the pellet was almost entirely comprised of dead cell mass (Fig. 6a, b, f–h). However, in contrast to seed medium, live mycelia started to appear in the core of pellets of nonproducing medium after 60 h and the fraction of live cells in the core as well as the live cells in peripheral mycelia increased from 60 to 72 h (Fig. 6h, j). This is followed by a second death phase, where the fraction of dead cells increases in the core with a concomitant decrease in the fraction of live peripheral mycelia (Fig. 6k, m, p, q). This was confirmed by confocal microscopy carried out at higher magnification which showed the presence of live cells in the core at 60 h but not at 120 and 168 h (Fig. 6i, o, r). Also, at 120 h, the peripheral region contained predominantly live mycelia (Fig. 6n). Further, similar to observation in seed medium as well as in high balhimycin producing medium, septation of hyphae did not vary with time in pellets of cultures having 1.0 g l^{-1} of KH_2PO_4 which did not produce balhimycin (Fig. 6e, l).

Altogether, the spatio-temporal distribution of live and dead cells in pellets of *A. balhimycina* showed marked differences when cultured in high balhimycin producing and nonproducing media containing 0.2 and 1.0 g l^{-1} of KH_2PO_4, respectively.

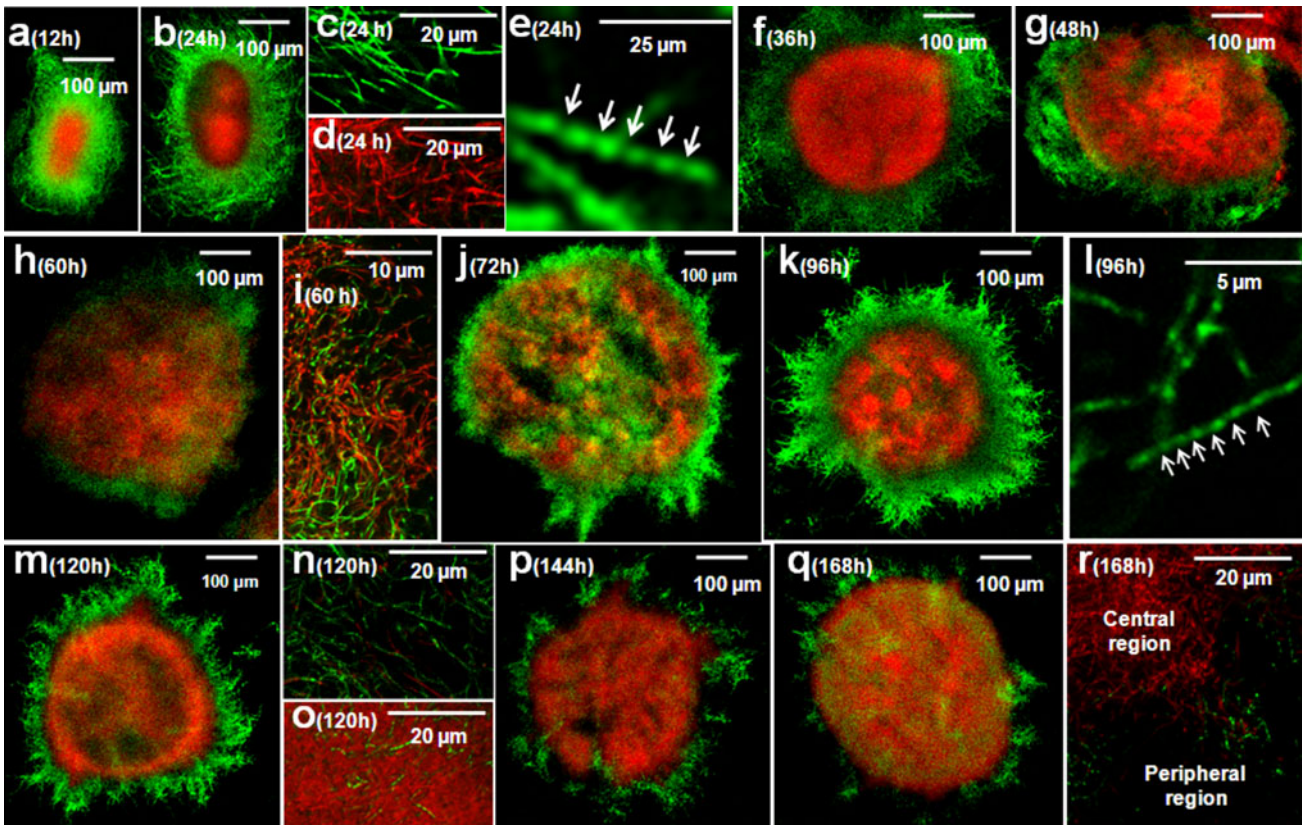

Fig. 6 Confocal micrographs of live and dead cells in pellets of *A. balhimycina* cultured in medium containing 1.0 g l^{-1} of KH_2PO_4. Samples were collected at 12 h intervals from the bioreactor and stained with SYTO 9 and PI to identify live and dead cells, respectively (details in "Materials and methods" section). *Sample time point* (hours) and *scale bar* (micrometers) are indicated in each figure (**a**–**r**). **c** and **n** represent mycelial structure from pellet periphery at 24 h (**b**) and 120 h (**m**), respectively. **d** and **o** represent central mycelial structure inside the pellet at 24 h (**b**) and 120 h (**m**), respectively. **i** represents mycelial structure at 60 h from central region of the pellet (**h**). **r** represents central and peripheral mycelial structure of pellet at 168 h (**q**). *Arrows* in **e** and **l** position of septa inside the live mycelia

Discussion

Some studies have reported that the differences in culture vessel geometry may lead to changes in morphology of filamentous micro-organisms [7, 34]. Therefore, we compared *A. balhimycina* growth, substrate consumption and balhimycin production for various media compositions in bioreactor fermentations to those in shake flask experiments and found that the profiles of *A. balhimycina* growth, substrate consumption and balhimycin production remain largely unchanged (Fig. 1). Moreover, the relative abundance of dispersed and pellet morphological forms in the bioreactor and shake flask showed similar trends in the bioreactor and shake flask experiments (Fig. 2). Furthermore, the pellet morphologies observed in bioreactor and shake flask experiments for various media compositions also did not differ (data not shown). Our data confirm that media composition, and not vessel geometry or fluid mechanical forces, was responsible for the observed differences.

The co-existence of a high fraction of dispersed phase and larger pellets in the media having high KH_2PO_4 concentration may be explained by the stronger shear forces experienced by highly exposed peripheral mycelia of larger pellets, resulting in breakage of these peripheral mycelia (Figs. 2, 6). Moreover, pellets in cultures with high KH_2PO_4 concentration undergo the first death phase after 48 h, which correlates with increased amount of dispersed mycelia, possibly due to breakage of large pellets (Figs. 2, 6). In contrast, peripheral mycelia of the small pellets in the media having low KH_2PO_4 concentration appear to be more compact and experience shear forces of smaller magnitudes, which may explain the relative scarcity of dispersed mycelia in the culture (Figs. 2, 5).

Live and dead cell imaging has been previously demonstrated in submerged cultivation of a sporulating strain of *S. coelicolor* that produced actinorhodin and undecylprodigiosin [20, 40]. For this strain, it was reported that the spores germinate to form initial compartmentalized mycelia, which subsequently form spherical pellets that

grow in a radial pattern [20]. It was also found that, following a first growth phase, a first death phase is initiated at the center of the pellets and this central core of dead cell mass grows radially [20]. Subsequently, a second growth phase is initiated by the appearance of secondary multinucleated mycelium within the pellet including the central core, which is responsible for undecylprodigiosin and actinorhodin production [20, 40]. Though *A. balhimycina* is a non-sporulating organism, we observe a similar set of morphological events in medium which did not support balhimycin production. In this medium containing 1.0 g l^{-1} of KH_2PO_4, after the primary death phase has progressed substantially, a secondary growth phase appears in the pellet including in the central core (Fig. 6). However, unlike *S. coelicolor* this was not accompanied by product formation (Fig. 1b). In fact, in the case of high balhimycin producing media containing 0.2 g l^{-1} of KH_2PO_4, *A. balhimycina* pellets did not exhibit the central core of dead cells or a secondary growth phase (Fig. 5). Interestingly, though the central core of dead cells was also observed within pellets of *A. balhimycina* grown in seed medium, secondary mycelia were absent (Fig. 4). Moreover, unlike pellets of *S. coelicolor* which exhibit secondary mycelia that are multinucleated [20], *A. balhimycina* pellets posses only compartmentalized mycelium throughout the entire culture duration in all three culture media (Figs. 4, 5, 6).

Recent proteome analysis of *S. coelicolor* development revealed that the onset of secondary metabolism coincides with hypha differentiation [24]. In fact, it was reported that the first compartmentalized mycelia, not involved in antibiotic production, had higher expression of enzymes associated with primary metabolism, while second multinucleated mycelia showed relatively proteins involved in secondary metabolism [24]. A differential proteomic comparison of two *A. balhimycina* bioreactor cultivations, one with low phosphate and high glucose medium leading to high balhimycin production rate and another having high phosphate and low glucose resulting in a low rate of balhimycin synthesis has been recently reported [13]. Interestingly, their analysis revealed increased synthesis of primary metabolites eventually required for biomass production and balhimycin synthesis [13]. Moreover, it was reported that up-regulation of central carbon metabolism enzymes did not result in an increased biomass production, due to phosphate limitation that negatively affected growth [13]. Further, it was proposed that differential expression of central carbon metabolism key enzymes led to the metabolic adaptation to energetic imbalance due to phosphate limitation [13]. Our data also suggest that phosphate limitation, responsible for growth inhibition and balhimycin synthesis, may also be implicated in morphological adaptation (Figs. 1, 5).

In conclusion, our work demonstrates that media composition significantly affects not only balhimycin production, but also modulates *A. balhimycina* pellet histology. Moreover, the nature of correlation between secondary metabolite production and morphology of *A. balhimycina* pellets is markedly different from previously reported results with *S. coelicolor*. A rigorous investigation of pellet morphology may provide important insights into the role of cellular differentiation and heterogeneity in secondary metabolite production.

Acknowledgments The authors gratefully acknowledge Dr. Anna Eliasson Lantz for providing *A. balhimycina* DSM 5908 and the balhimycin standard. The work was partially supported by grants from the Department of Biotechnology, Ministry of Science and Technology, Government of India awarded to PPW and the Department of Science and Technology, Ministry of Science and Technology, Government of India awarded to SJ. KPS acknowledges fellowship from University Grants Commission, Government of India.

References

1. Allen NE, LeTourneau DL, Hobbs JN (1997) The role of hydrophobic side chains as determinants of antibacterial activity of semisynthetic glycopeptide antibiotics. J Antibiot 50(8):677–684
2. Bapat PM, Bhartiya S, Venkatesh KV, Wangikar PP (2006) Structured kinetic model to represent the utilization of multiple substrates in complex media during rifamycin B fermentation. Biotechnol Bioeng 93(4):779–790. doi:10.1002/bit.20767
3. Bapat PM, Padiyar NU, Dave NN, Bhartiya S, Wangikar PP, Dash S (2006) Model-based optimization of feeding recipe for rifamycin fermentation. AIChE J 52(12):4248–4257. doi:10.1002/aic.11034
4. Bapat PM, Wangikar PP (2004) Optimization of rifamycin B fermentation in shake flasks via a machine-learning-based approach. Biotechnol Bioeng 86(2):201–208
5. Berdy J (2005) Bioactive microbial metabolites—a personal view. J Antibiot 58(1):1–26
6. Bibb MJ (2005) Regulation of secondary metabolism in *Streptomycetes*. Curr Opin Microbiol 8(2):208–215. doi:10.1016/j.mib.2005.02.016
7. Braun S, Vechtlifshitz SE (1991) Mycelial morphology and metabolite production. Trends Biotechnol 9(2):63–68
8. Collins TJ (2007) ImageJ for microscopy. Biotechniques 43(1 Suppl):25–30
9. Demain AL, Fang A (1995) Emerging concepts of secondary metabolism in actinomycetes. Actinomycetologica 9:98–117
10. Dobson LF, O'Cleirigh CC, O'Shea DG (2008) The influence of morphology on geldanamycin production in submerged fermentations of *Streptomyces hygroscopicus* var. geldanus. Appl Microbiol Biotechnol 79(5):859–866. doi:10.1007/s00253-008-1493-3
11. Fernandez M, Sanchez J (2001) Viability staining and terminal deoxyribonucleotide transferase-mediated dUTP nick end labelling of the mycelium in submerged cultures of *Streptomyces antibioticus* ETH7451. J Microbiol Methods 47(3):293–298
12. Fernandez M, Sanchez J (2002) Nuclease activities and cell death processes associated with the development of surface cultures of *Streptomyces antibioticus* ETH 7451. Microbiology 148(2):405–412
13. Gallo G, Alduina R, Renzone G, Thykaer J, Bianco L, Eliasson-Lantz A, Scaloni A, Puglia AM (2010) Differential proteomic

analysis highlights metabolic strategies associated with balhimycin production in *Amycolatopsis balhimycina* chemostat cultivations. Microb Cell Fact 9:95. doi:10.1186/1475-2859-9-95
14. Hongjuan Z, Parry RL, Ellis EI, Griffith GW, Goodacre R (2006) The rapid differentiation of *Streptomyces* isolates using Fourier transform infrared spectroscopy. Vib Spectrosc 40:213–218
15. Jonsbu E, McIntyre M, Nielsen J (2002) The influence of carbon sources and morphology on nystatin production by *Streptomyces noursei*. J Biotechnol 95(2):133–144
16. Komives C, Parker RS (2003) Bioreactor state estimation and control. Curr Opin Biotechnol 14(5):468–474. doi:10.1016/j.copbio.2003.09.001
17. Lawton P, Whitaker A, Odell D, Stowell JD (1989) Actinomycete morphology in shaken culture. Can J Microbiol 35(9):881–889
18. Maiti SK, Singh KP, Lantz AE, Bhushan M, Wangikar PP (2010) Substrate uptake, phosphorus repression, and effect of seed culture on glycopeptide antibiotic production: process model development and experimental validation. Biotechnol Bioeng 105(1):109–120. doi:10.1002/bit.22505
19. Maiti SK, Srivastava RK, Bhushan M, Wangikar PP (2009) Real time phase detection based online monitoring of batch fermentation processes. Process Biochem 44(8):799–811. doi:10.1016/j.procbio.2009.03.008
20. Manteca A, Alvarez R, Salazar N, Yague P, Sanchez J (2008) Mycelium differentiation and antibiotic production in submerged cultures of *Streptomyces coelicolor*. Appl Environ Microbiol 74(12):3877–3886. doi:10.1128/Aem.02715-07
21. Manteca A, Claessen D, Lopez-Iglesias C, Sanchez J (2007) Aerial hyphae in surface cultures of *Streptomyces lividans* and *Streptomyces coelicolor* originate from viable segments surviving an early programmed cell death event. FEMS Microbiol Lett 274(1):118–125. doi:10.1111/j.1574-6968.2007.00825.x
22. Manteca A, Fernandez M, Sanchez J (2005) A death round affecting a young compartmentalized mycelium precedes aerial mycelium dismantling in confluent surface cultures of *Streptomyces antibioticus*. Microbiology 151(11):3689–3697. doi:10.1099/mic.0.28045-0
23. Manteca A, Fernandez M, Sanchez J (2005) Mycelium development in *Streptomyces antibioticus* ATCC11891 occurs in an orderly pattern which determines multiphase growth curves. BMC Microbiol 5:51. doi:10.1186/1471-2180-5-51
24. Manteca A, Jung HR, Schwammle V, Jensen ON, Sanchez J (2010) Quantitative proteome analysis of *Streptomyces coelicolor* non-sporulating liquid cultures demonstrates a complex differentiation process comparable to that occurring in sporulating solid cultures. J Proteome Res 9(9):4801–4811. doi:10.1021/pr100513p
25. Manteca A, Mäder U, Connolly BA, Sanchez J (2006) A proteomic analysis of *Streptomyces coelicolor* programmed cell death. Proteomics 6(22):6008–6022. doi:10.1002/pmic.200600147
26. Manteca A, Sanchez J (2009) *Streptomyces* development in colonies and soils. Appl Environ Microbiol 75(9):2920–2924. doi:10.1128/Aem.02288-08
27. Martin JF (2004) Phosphate control of the biosynthesis of antibiotics and other secondary metabolites is mediated by the PhoR-PhoP system: an unfinished story. J Bacteriol 186(16):5197–5201. doi:10.1128/Jb.186.16.5197-5201.2004
28. Martin JF, Demain AL (1980) Control of antibiotic biosynthesis. Microbiol Rev 44(2):230–251
29. Mason MG, Ball AS, Reeder BJ, Silkstone G, Nicholls P, Wilson MT (2001) Extracellular heme peroxidases in actinomycetes: a case of mistaken identity. Appl Environ Microbiol 67(10):4512–4519
30. McCarthy AJ (1987) Lignocellulose-degrading actinomycetes. FEMS Microbiol Lett 46(2):145–163. doi:10.1111/j.1574-6968.1987.tb02456.x
31. Morrison GR (1971) Microchemical determination of organic nitrogen with nessler reagent. Anal Biochem 43:527–532
32. Nadkarni SR, Patel MV, Chatterjee S, Vijayakumar EKS, Desikan KR, Blumbach J, Ganguli BN, Limbert M (1994) Balhimycin, a new glycopeptide antibiotic produced by *Amycolatopsis* sp. Y-86,21022—taxonomy, production, isolation and biological-activity. J Antibiot 47(3):334–341
33. O'Cleirigh C, Casey JT, Walsh PK, O'Shea DG (2005) Morphological engineering of *Streptomyces hygroscopicus* var. geldanus: regulation of pellet morphology through manipulation of broth viscosity. Appl Microbiol Biotechnol 68(3):305–310. doi:10.1007/s00253-004-1883-0
34. Papagianni M, Mattey M (2006) Morphological development of *Aspergillus niger* in submerged citric acid fermentation as a function of the spore inoculum level. Application of neural network and cluster analysis for characterization of mycelial morphology. Microb Cell Fact 5:3. doi:10.1186/1475-2859-5-3
35. Sathi Z, Sultana MD, Aziz AR, Gafur MA (2001) Identification and in vitro antimicrobial activity of a compound isolated from *Streptomyces* sp. Pak J Biol Sci 12:1523–1525
36. Singh KP, Wangikar PP, Jadhav S (2012) Correlation between pellet morphology and glycopeptide antibiotic balhimycin production by *Amycolatopsis balhimycina* DSM 5908. J Ind Microbiol Biotechnol 39(1):27–35. doi:10.1007/s10295-011-0995-7
37. Tang JS, Gillevet PM (2003) Reclassification of ATCC 9341 from *Micrococcus luteus* to *Kocuria rhizophila*. Int J Syst Evol Microbiol 53(Pt 4):995–997
38. Vanimpe JF, Bastin G (1995) Optimal adaptive-control of fed-batch fermentation processes. Contr Eng Pract 3(7):939–954
39. Whitaker A (1992) Actinomycetes in submerged culture. Appl Biochem Biotechnol 32:23–35
40. Yague P, Manteca A, Simon A, Diaz-Garcia ME, Sanchez J (2010) New method for monitoring programmed cell death and differentiation in submerged *Streptomyces* cultures. Appl Environ Microbiol 76(10):3401–3404. doi:10.1128/AEM.00120-10
41. Yin P, Wang YH, Zhang SL, Chu J, Zhuang YP, Chen N, Li XF, Wu YB (2008) Effect of mycelial morphology on bioreactor performance and avermectin production of *Streptomyces avermitilis* in submerged cultivations. J Chin Inst Chem Eng, 39(6):609–615. doi:10.1016/j.jcice.2008.04.008
42. Zhu CH, Lu FP, He YN, Han ZL, Du LX (2007) Regulation of avilamycin biosynthesis in *Streptomyces viridochromogenes*: effects of glucose, ammonium ion, and inorganic phosphate. Appl Microbiol Biotechnol 73(5):1031–1038. doi:10.1007/s00253-006-0572-6